10264 *Inorg. Chem.* **2009**, *48*, 10264–10274
DOI: 10.1021/ic901379d

Inorganic Chemistry
Article

Building Multistate Redox-Active Architectures Using Metal-Complex Functionalized Perylene Bis-imides

Gudrun Goretzki,[†] E. Stephen Davies,[†] Stephen P. Argent,[†] John E. Warren,[‡] Alexander J. Blake,[†] and Neil R. Champness*,[†]

[†]*School of Chemistry, University of Nottingham, University Park, Nottingham NG7 2RD, U.K., and* [‡]*Daresbury Laboratory, Synchrotron Radiation Source, Warrington WA4 4AD, U.K.*

Received July 14, 2009

A series of multistate redox-active architectures has been synthesized, structurally characterized, and their optical and redox properties investigated. Specifically, two redox-active ferrocene or cobalt-dithiolene moieties have been introduced to the "bay" region of perylene-bisimides. Three of these disubstituted perylene-bisimide species have been structurally characterized by single crystal X-ray diffraction, confirming the twisted nature of the central perylene core. The first isomeric pair of disubstituted perylene-bisimide isomers, *N*,*N*′-di-(*n*-butyl)-1,7-diferrocenyl-perylene-3,4:9,10-tetracarboxylic acid bisimide (**2**) and *N*,*N*′-di-(*n*-butyl)-1,6-diferrocenyl-perylene-3,4:9,10-tetracarboxylic acid bisimide (**3**), structurally characterized by single crystal X-ray diffraction are reported and compared. Structural characterization of the cobalt-dithiolene substituted perylene-bisimide, *N*,*N*′-di-(*n*-butyl)-1,7-dicyclopentadienyl-cobalt(II)-dithiolenyl-perylene-3,4:9,10-tetracarboxylic acid bisimide (**4**), reveals the expected twisting of the perylene core and confirms the ene-dithiolate geometry of the cobalt dithiolene moiety. Cyclic voltammetry measurements, coupled with spectroelectrochemcial and electron paramagnetic resonance studies, of **1**−**4**, where **1** is *N*,*N*′-di-(*n*-butyl)-1,7-diethynylferrocenyl-perylene-3,4:9,10-tetracarboxylic acid bisimide, reveal the two anticipated perylene-bisimide based reductions. In addition, for the ferrocene substituted compounds, **1**−**3**, a single reversible two-electron oxidation is seen with only a small degree of communication between the ferrocene groups observed in the 1,6-isomer where the two ferrocene groups are attached to the same naphthyl moiety. In the case of **4**, two reversible reductions associated with the cobalt-dithiolene moieties are observed, confirming communication across the reduced perylene core.

Introduction

The design of species for storing information at the molecular or submolecular scale represents one of the major challenges for molecular nanoscience.[1] Such information storage may be achieved in a number of ways but perhaps the most readily targeted multistate systems are those that allow switching between molecular redox states.[2] Indeed, if reversible switching is possible in such systems it may be possible to develop molecular units capable of adopting a number of different states that can be probed by a variety of techniques. In particular, by appropriate choice of component, redox states can be assessed by electrochemical, magnetic, electron paramagnetic resonance (EPR), or spectroscopic methods.

Perylene-bisimides and their derivatives have received a great deal of attention because of their remarkable electrochemical and optical properties,[3] and they are potentially attractive targets for molecular species capable of information storage. Their properties have been exploited for a number of applications including n-type semiconductors,[4] thin film-transistors,[5] and in solar cells.[6] In addition, the extended aromatic structure of the perylene core coupled with extensive scope for derivatization makes them attractive

*To whom correspondence should be addressed. E-mail: neil.champness@nottingham.ac.uk. Phone: +44 115 951 3505. Fax +44 115 9513563.

(1) Joachim, C.; Gimzewski, J. K.; Aviram, A. *Nature* **2000**, *408*, 541–548. Pease, A. R.; Jeppesen, J. O.; Stoddart, J. F.; Luo, Y.; Collier, C. P.; Heath, J. R. *Acc. Chem. Res.* **2001**, *34*, 433–444. Service, R. F. *Science* **2001**, *293*, 782–785.

(2) Ruben, M.; Breuning, E.; Gisselbrecht, J. P.; Lehn, J.-M. *Angew. Chem., Int. Ed.* **2000**, *39*, 4139–4142. Ruben, M.; Lehn, J.-M.; Müller, P. *Chem. Soc. Rev.* **2006**, *35*, 1056–1067.

(3) Würthner, F. *Chem. Commun.* **2004**, 1564–1579.

(4) (a) Struijk, C. W.; Sieval, A. B.; Dakhorst, J. E. J.; Van Dijk, M.; Kimkes, P.; Koehorst, R. B. M.; Donker, H.; Schaafsma, T. J.; Picken, S. J.; Van de Craats, A. M.; Warman, J. M.; Zuilhof, H.; Sudhölter, E. J. R. *J. Am. Chem. Soc.* **2000**, *122*, 11057–11066. (b) Dimitrakopoulos, C. D.; Malenfant, P. R. L. *Adv. Mater.* **2002**, *14*, 99–117. (c) Langhals, H. *Heterocycles* **1995**, *40*, 477. (d) Yoo, B.; Jung, T.; Basu, D.; Dodabalapur, A.; Jones, B. A.; Faccetti, A.; Wasielewski, M. R.; Marks, T. J. *Appl. Phys. Lett.* **2006**, *88*, 082104.

(5) (a) Würthner, F. *Angew. Chem., Int. Ed.* **2001**, *40*, 1037–1039. (b) Jones, B. A.; Facchetti, A.; Wasielewski, M. R.; Marks, T. J. *Adv. Funct. Mater.* **2008**, *18*, 1329–1339.

(6) Ferrere, S.; Zaban, A.; Gregg, B. A. *J. Phys. Chem. B* **1997**, *101*, 4490–4493.

 Published on Web 10/02/2009

targets for the generation of liquid crystals[7] and for surface-based self-assembly processes.[8]

Perylene-bisimides typically display two reversible reduction processes[3,7,9] accompanied by a variety of color changes[10] and, in some instances, switching of fluorescence properties.[11] Bearing in mind the rich electrochemical properties of the extensive aromatic perylene-bisimide subunit, it is perhaps surprising that they have not been developed as components for the burgeoning field of molecules capable of information storage. However, if chemical derivatization is considered it becomes more apparent why this is the case. The most facile synthetic strategy for derivatization of perylenetetracarboxylic bisimides is via variation in amine appendage utilized in the initial formation of the imide moiety. Such functionalization is readily achieved but has limited influence upon the electronic and optical properties of the aromatic perylene core.[12] Molecular orbital calculations on such compounds reveal a node in the highest occupied molecular orbital (HOMO) at the nitrogen atoms of the two imide functions and this precludes the use of appendages to the imides for electronic communication pathways. Alternatively, derivatization can be achieved in the "bay region" at the 1, 6, 7, and/or 12 positions of the perylene core. Although synthetically more complex, such reactions have the advantage that appended functional groups are directly attached to the perylene core, a situation which may be anticipated to facilitate orbital overlap between the appendage and the aromatic core of the molecule, potentially resulting in communication across the molecule. Although a wide variety of functionalized perylenetetracarboxylic bisimides is possible, attachment of appendages to the perylene core in the bay region is anticipated to result in twisting of the two naphthyl moieties of the perylene core linked at the 13/14 and 17/18 positions.[3,10b] Although not entirely prohibitive, distortion of the perylene core may be anticipated to inhibit communication across this moiety reducing the interaction between redox groups on opposing sides of the perylene moiety.

We have targeted three related molecular species that contain redox active metal complex based appendages to the central *N*,*N*′-di-(*n*-butyl)-3,4:9,10-tetracarboxylic acid bisimide (PBI) core. In particular, a series of molecules has been prepared: 1,7-$(C{\equiv}CFc)_2$-PBI **1**, two isomers of ferrocenyl (Fc) substituted PBI, 1,7-$(Fc)_2$-PBI **2** and 1,6-$(Fc)_2$-PBI **3**, and a cyclopentadienyl cobalt dithiolene functionalized species 1,7-$[(cp)Co(II)S_2C_2H]_2$-PBI **4** (Scheme 1). Compounds **1**−**4** are among the first examples of perylenetetracarboxylic bisimides functionalized with redox active groups. Previous examples of ferrocene functionalized PBIs,[10a,11] in which the redox active appendages are separated from the perylene core by a non-conjugated linker, would not be anticipated to, and do not provide direct electrochemical communication to the perylene core.

Experimental Section

Synthetic Methodology. Perylene-3,4:9,10-tetracarboxylic acid (Aldrich) was used as starting material for the synthesis of 1,7-dibromo-perylene-3,4:9,10-tetracarboxylic acid[13] and *N*,*N*′-bis-(*n*-butyl)-1,7-dibromo-3,4:9,10-perylenetetracarboxylic bisimide.[13] Ethynylferrocene[14] and $[NBu_4][BF_4]$[15] were prepared by literature methods. Ferrocenylboronic acid was purchased from Aldrich and used as supplied. All reactions were carried out under an atmosphere of dinitrogen or argon where noted. Column chromatography was performed on silica gel (Merck silica gel 60, 0.2−0.5 mm, 50−130 mesh). It is known that the bromination of perylene bis-anhydride affords a mixture of 1,7- and 1,6-isomers, typically is the ratio 80:20.[13] Although the different isomers could be detected via NMR spectroscopy throughout the synthetic path, separation on the large scale could not be accomplished and, unless otherwise stated, the isomeric mixtures were used. ^{1}H NMR (300 MHz) and ^{13}C NMR (75 MHz) were obtained on a Bruker 300 MHz spectrometer. Microanalyses were performed by Stephen Boyer, London Metropolitan University, London, U.K. MS spectra (MALDI-TOF-MS) were determined on a Voyager-DE-STR mass spectrometer.

***N*,*N*′-Di-(*n*-butyl)-1,7-Di-(trimethylsilylethynylen)perylene-3,4:9,10-tetracarboxylic Acid Bisimide.** *N*,*N*′-di-(*n*-butyl)-1,7-dibromoperylene-3,4:9,10-tetracarboxylic acid bisimide[13] (3 mmol) was dissolved in a mixture of dry tetrahydrofuran (THF, 100 mL) and dry triethylamine (50 mL) in an Ar atmosphere. $PdCl_2(PPh_3)_2$ (84 mg, 0.12 mmol), CuI (29 mg, 0.15 mmol), and ethynyltrimethylsilane (1.66 mL, 12 mmol) were added, and the reaction mixture was stirred at 80 °C for 4 h, cooled to room temperature, and poured into 100 mL of cold diluted HCl. The product was extracted with CH_2Cl_2, and the organic layer washed with water until neutral. The crude product was purified by column chromatography on silica ($CHCl_3$) to give 1.68 g (89%) of a red powder. ^{1}H NMR ($CDCl_3$): δ = 10.17 (d, 2H, ^3J = 8.27); 8.82 (s, 2H); 8.62 (d, 2H, ^3J = 8.27); 4.25 (t, 4H, NCH_2, ^3J = 7.5 Hz); 1.78 (m, 4H); 1.49 (m, 4H); 1.02 (t, 6H, ^3J = 7.3 Hz); 0.41 (s, 18H). ^{13}C NMR ($CDCl_3$): δ = 163.18, 162.4288, 138.39, 138.03, 134.23, 133.93, 133.32, 130.40, 130.05, 127.56, 127,29, 123.51, 123.16, 122.0, 120.36, 119.80, 106.49, 105.62, 40.51, 30.23, 20.45, 13.95, −0.28. Anal. Calcd for $C_{42}H_{42}N_2O_4Si_2$: C: 72.59 ;H: 6.09; N: 4.03%; Found: C: 72.70; H: 6.15; N:3.98%. MS (EI): *m*/*z* 694.3 (M^+).

***N*,*N*′-Di-(*n*-butyl)-1,7-diethynylenperylene-3,4:9,10-tetracarboxylic Acid Bisimide.** *N*,*N*′-di-(*n*-butyl)-1,7-Di-(trimethylsilylethynylen)perylene-3,4:9,10-tetracarboxylic acid bisimide 1.39 g (2 mmol) was dissolved in $CHCl_3$ (75 mL) and MeOH (20 mL). NaOH (0.72 mmol, 29 mg) was added, and the reaction mixture was stirred at room temperature for 1 h. $CHCl_3$ was

(7) Wurthner, F.; Thalacker, C.; Diele, S.; Tschierske, C. *Chem.—Eur. J.* **2001**, *7*, 2245–2253.

(8) (a) Theobald, J. A.; Oxtoby, N. S.; Phillips, M. A.; Champness, N. R.; Beton, P. H. *Nature* **2003**, *424*, 1029. (b) Swarbrick, J. C.; Ma, J.; Theobald, J. A.; Oxtoby, N. S.; O'Shea, J. N.; Champness, N. R.; Beton, P. H. *J. Phys. Chem. B* **2005**, *109*, 12167. (c) Theobald, J. A.; Oxtoby, N. S.; Champness, N. R.; Beton, P. H.; Dennis, T. J. S. *Langmuir* **2005**, *21*, 2038. (d) Perdigão, L. M. A.; Perkins, E. W.; Ma, J.; Staniec, P. A.; Rogers, B. L.; Champness, N. R.; Beton, P. H. *J. Phys. Chem. B* **2006**, *110*, 12539. (e) de Feyter, S.; Miura, A.; Yao, S.; Chen, Z.; Würthner, F.; Jonkheijm, P.; Schenning, A. P. H. J.; Meijer, E. W.; de Schryver, F. C. *Nano Lett.* **2005**, *5*, 77. (f) Perdigao, L. M. A.; Saywell, A.; Fontes, G. N.; Staniec, P. A.; Goretzki, G.; Phillips, A. G.; Champness, N. R.; Beton, P. H. *Chem.—Eur. J.* **2008**, *14*, 7600.

(9) (a) You, C.; Espindola, P.; Hippius, C.; Heinze, J.; Würthner, F. *Adv. Funct. Mat.* **2007**, *17*, 3764–3772. (b) Ahrens, M. J.; Fuller, M. J.; Wasielewski, M. R. *Chem. Mater.* **2003**, *15*, 2684–2686. (c) Salbeck, J.; Kunkely, H.; Langhals, H.; Saalfrank, R. W.; Daub, J. *Chimia* **1989**, *43*, 6–9. (d) Chen, Z.; Debije, M. G.; Debaerdemaeker, T.; Osswald, P.; Würthner, F. *ChemPhysChem* **2004**, *5*, 137–140.

(10) (a) You, C.; Würthner, F. *J. Am. Chem. Soc.* **2003**, *125*, 9716–9725. (b) Goretzki, G.; Davies, E. S.; Argent, S. P.; Alsindi, W.; Blake, A. J.; Warren, J. E.; McMaster, J.; Champness, N. R. *J. Org. Chem.* **2008**, *73*, 8808.

(11) (a) Zhang, R.; Wang, Z.; Wu, Y.; Fu, H.; Yao, J. *Org. Lett.* **2008**, *10*, 3065–3068. (b) Huang, J.; Wu, Y.; Fu, H.; Zhan, X.; Yao, J.; Barlow, S.; Marder, S. R. *J. Phys. Chem. A* **2009**, *113*, 5039–5046.

(12) Langhals, H.; Demmig, S.; Huber, H. *Spectrochim. Acta* **1988**, *44A*, 1189–1193.

(13) Würthner, F.; Stepanenko, V.; Chen, Z.; Saha-Möller, C. R.; Kocher, N.; Stalke, D. *J. Org. Chem.* **2004**, *69*, 7933.

(14) Rosenblum, M.; Brawn, N.; Papenmeier, J.; Applebaum, M. J. *J. Organomet. Chem.* **1966**, *6*, 173.

(15) Kubas, J. *Inorg. Synth.* **1990**, *28*, 68.

Scheme 1. Synthetic Procedures for **1**, **4**, and **5**[a]

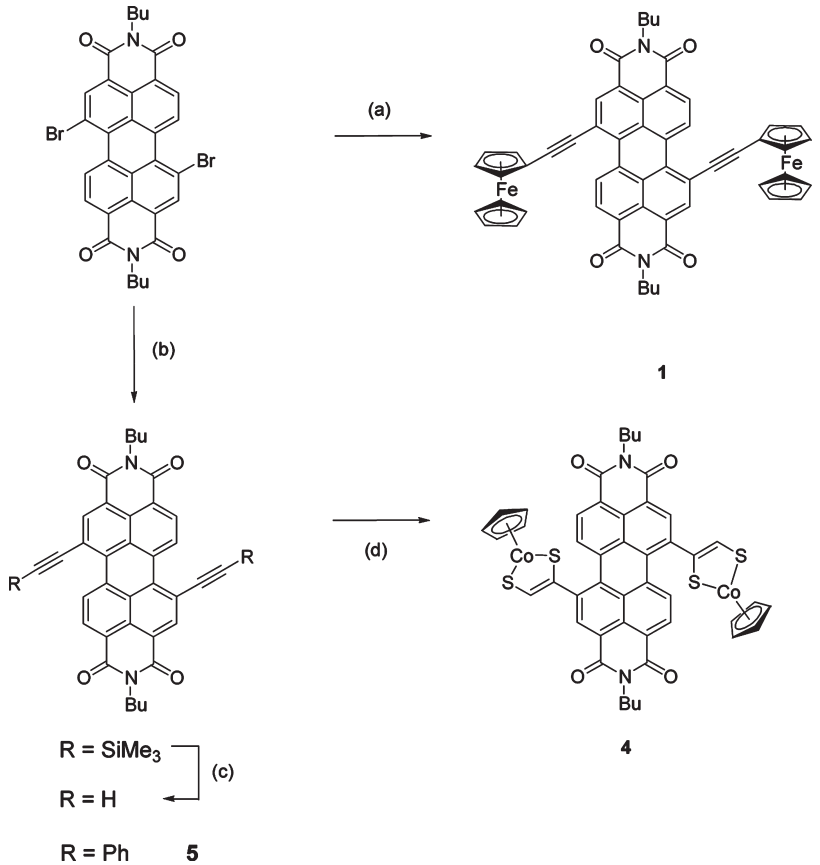

[a] (a) Fc-C≡CH, $Pd(PPh_3)_2Cl_2$, CuI, NEt_3, toluene, 110 °C, 76%; (b) THF, NEt_3, ethynyltrimethylsilane, $PdCl_2(PPh_3)_2$, CuI, 70°C, 89%; (c) MeOH/$CHCl_3$, NaOH, 95%; (d) S_8, cyclopentadienyl cobalt(I) dicarbonyl, toluene, 110°C, 63%. A mixture of both 1,7- and 1,6-Br_2−PBI was used in reactions (a) and (b) with any residual 1,6-isomers removed during purification procedures.

added to dissolve the product completely, and the NaOH removed by filtration. Precipitation with methanol yielded the product in quantitative yield and pure enough to be used in the next step without further purification. Acquisition of a ^{13}C NMR spectrum was precluded by the poor solubility of the compound. ^1H NMR ($CDCl_3$): δ = 10.22 (d, 2H, ^3J = 8.10 Hz); 8.95 (s, 2H); 8.82 (d, 2H, ^3J = 8.10 Hz); 4.29 (t, 4H, ^3J = 7.5 Hz); 3.94 (s, 2H); 1.76 (m, 4H); 1.49 (m, 4H), 1.01 (t, 6H, ^3J = 7.3 Hz). Anal. Calcd for $C_{36}H_{26}N_2O_4$: C: 78.53; H: 4.76; N: 5.09%. Found: C:78.60; H: 4.83; N: 4.98%. MS (MALDI-TOF): m/z 550.2 (M^+).

***N,N′*-Di-(*n*-butyl)-1,7-diethynylferrocenyl-perylene-3,4:9,10-tetracarboxylic Acid Bisimide 1.** *N,N′*-Di-(*n*-butyl)-1,7-dibromoperylene-3,4:9,10-tetracarboxylic acid bisimide[13] (0.66 g, 1 mmol) was dissolved in a mixture of dry toluene (100 mL) and dry triethylamine (50 mL) in an Ar atmosphere. $PdCl_2(PPh_3)_2$ (70 mg, 0.1 mmol), CuI (22 mg, 0.11 mmol), and ethynylferrocene[14] (0.46 g, 2.2 mmol) were added, and the reaction mixture was stirred at 70 °C for 8 h. Following cooling to room temperature, the product was extracted with CH_2Cl_2 and filtered through a small silica pad. The crude product was purified by recrystallization from $CHCl_3$ and MeOH to give 0.70 g (76%) of a red powder.

^1H NMR ($CDCl_3$): δ = 10.13 (d, 2H, ^3J = 7.74); 8.81 (s, 2H); 8.72 (d, 2H, ^3J = 7.74), 4.72 (s, 4H, Fc), 4.5 (s, 4H, Fc), 4.36 (s, 10H, Fc), 4.26 (t, 4H, ^3J = 7.5 Hz), 1.78 (m, 4H), 1.48 (m, 4H), 1.04 (t, 6H, ^3J = 7.3 Hz). ^{13}C NMR ($CDCl_3$): δ = 163.39, 163.11, 137.40, 134.23, 132.97, 129.83, 127.69, 127.20, 126.50, 122.77, 121.82, 120.78, 100.75, 88.13, 71.93, 70.42, 70.30, 63.66, 40.48, 30.98, 30.26, 20.46, 13.94. We were unable to obtain meaningful CHN data because of incomplete combustion of **1**. MS (MALDI-TOF): m/z 918.2 (M^+). *N,N′*-Di-(*n*-octyl)-1,7-diethynylferrocenyl-perylene-3,4:9,10-tetracarboxylic acid bisimide **1a** was prepared in an analogous fashion to **1** but using *N,N′*-di-(*n*-octyl)-1,7-dibromoperylene-3,4:9,10-tetracarboxylic acid bisimide as a starting material. **1a** ^1H NMR ($CDCl_3$): δ = 10.16 (d, 2H, ^3J = 6.3 Hz); 8.84 (s, 2H); 8.73 (d, 2H, ^3J = 6.3 Hz), 4.72 (s, 4H, Fc), 4.49 (s, 4H, Fc), 4.35 (s, 10H, Fc), 4.28 (t, 4H, ^3J = 7.5 Hz), 1.79 (m, 4H), 1.48 (m, 20H), 0.91 (t, 6H, ^3J = 7.3 Hz).

***N,N′*-Di-(*n*-butyl)-1,7-diferrocenyl-perylene-3,4:9,10-tetracarboxylic Acid Bisimide 2 and *N,N′*-Di-(*n*-butyl)-1,6-diferrocenyl-perylene-3,4:9,10-tetracarboxylic Acid Bisimide 3**. *N,N′*-Bis-(*n*-butyl)-1,7-dibromo-3,4:9,10-perylenetetracarboxylic bisimide[13] (mixture of isomers, 297 mg, 0.45 mmol), ferrocenylboronic acid (310 mg, 1.35 mmol), CsF (274 mg, 1.8 mmol), Ag_2O (232 mg, 1 mmol), and $Pd(PPh_3)_4$ (26 mg, 0.022 mmol) were dissolved in dry THF (70 mL) and the solution degassed. After stirring at 80 °C for 24 h the solvent was removed under reduced pressure, and the residue subjected to column chromatography on silica with CH_2Cl_2 to yield the desired product as a red powder in 35% yield. The 1,7- (**2**) and 1,6- (**3**) were separated on a smaller scale by column chromatography using CH_2Cl_2 as eluent on silica.

2: ^1H NMR ($CDCl_3$): δ = 9.02 (s, 2H), 8.16 (d, 2H, ^3J = 8.17 Hz), 7.82 (d, 2H, ^3J = 8.17 Hz), 4.55 (dd, 8H, FcH), 4.22 (m, 14H, NCH_2-butyl + FcH), 1.76 (m, 4H), 1.48 (m, 4H), 1.01 (t, 6H, ^3J = 7.5 Hz), ^{13}C NMR ($CDCl_3$): δ = 163.87, 163.73, 138.54, 136.42, 134.24, 133.29, 129.1, 128.67, 128.52, 126.99, 121.52, 120.52, 89.61, 70.58, 70.33, 70.25, 40.55, 30.38, 20.56, 13.98. Anal. Calcd for $C_{52}H_{42}N_2O_4Fe_2$: C: 71.74; H: 4.86; N: 3.21%. Found: C: 71.75; H: 4.77; N: 3.18%. MS (MALDI-TOF): m/z 870.2 (M^+).

3: ^1H NMR ($CDCl_3$): δ = 9.13 (s, 2H), 8.23 (d, 2H, ^3J = 8.08 Hz), 7.87 (d, 2H, ^3J = 8.08 Hz), 4.49 + 4.40 (dt, 4H each), 4.27 (t, 4H, ^3J = 7.5 Hz), 4.17 (s, 10H), 1.81, (m, 2H)), 1.72 (m, 2H),

1.46 (m, 4H), 1.04 (t, 3H, ^3J = 7.3 Hz). ^{13}C NMR ($CDCl_3$): δ = 163.91, 163.72, 138.53, 136.44, 134.32 133.36, 129.11, 128.72, 128.55, 127.03, 121.53 120.55, 89.51, 70.49, 70.25, 70.21, 40.49, 30.34, 20.52 13.94; MS (MALDI-TOF): m/z 870.2 (M^+).

***N,N′*-Di-(*n*-butyl)-1,7-dicyclopentadienyl-cobalt(II)-dithiolenyl-perylene-3,4:9,10-tetracarboxylic Acid Bisimide 4.** A mixture of *N*,*N*′-di-(*n*-butyl)-1,7-diethynylenperylene-3,4:9,10-tetracarboxylic acid bisimide (55 mg, 0.1 mmol), cyclopentadienyl cobalt(I) dicarbonyl (39 mg, 0.216 mmol) and sulfur (13 mg, 0.41 mmol) in degassed toluene (30 mL) was stirred under reflux for 30 h. The solvent was removed under reduced pressure and the residue purified by column chromatography (CH_2Cl_2) to yield the product as a dark blue in 63% yield.

^{1}H NMR ($CDCl_3$): δ = ^{1}H NMR ($CDCl_3$): δ = 8.77 (s, 2H, thiane), 8.64 (s, 2H), 7.95 (d, 2H, ^3J = 8.18 Hz), 7.08 (d, 2H, ^3J = 8.18 Hz), 5.48 (s, 10H, Cp-H), 4.18 (t, 4H, ^3J = 7.5 Hz), 1.72, (m, 4H)), 1.43 (m, 4H), 0.99 (t, 6H, ^3J = 7.3 Hz); ^{13}C NMR ($CDCl_3$): δ = 163.57, 163.30, 157.77, 140.09, 137.64, 135.89, 134.99, 134.49, 131.96, 130.08, 129.41, 128.86, 127.76, 121.76, 121.65, 79.79, 40.32, 30.26, 20.40, 13.90. Anal. Calcd for $C_{40}H_{40}N_4O_6$: C: 59.61; H: 3.91; N: 3.01%;. Found: C: 59.53; H: 3.86; N: 2.94%; MS (MALDI-TOF): m/z 926 (M^+).

Single Crystal X-ray Diffraction Studies. Single crystal X-ray data for **2** were collected on an Enraf-Nonius KappaCCD area detector diffractometer (rotating anode, graphite Mo-K_α radiation λ = 0.71073 Å) or, for **3** and **4**, on a Bruker SMART APEXII CCD area detector diffractometer at Station 9.8 of the Daresbury Laboratory Synchrotron Radiation Source (λ = 0.6911 Å).[16] The crystals were cooled using an Oxford Cryosystems cryostat.[17] The structures were solved by direct methods using SHELXS97;[18] subsequent full-matrix least-squares refinement employed SHELXL97.[18] All hydrogen atoms were placed in geometrically calculated positions and thereafter refined using a riding model with U_{iso}(H) = 1.2U_{eq}(C). All non-hydrogen atoms were refined with anisotropic displacement parameters. For **2** the crystal was found to be non-merohedrally twinned by 180° rotation about the [−203] reciprocal lattice direction: the twin fraction refined to 0.346(3). Geometric restraints were applied to the bond lengths of the imide portions of one of the two molecules found in the asymmetric unit, (Fe3/Fe4 C1B−C64B). Geometric restraints were applied to the 1,2 and 1,3 bond lengths of all four butyl chains. All non-hydrogen atoms were refined anisotropically with appropriate restraints (SIMU, DELU)[18] applied to all displacement parameters. Small electron density peaks near the bay regions of molecule B (Fe3/Fe4 C1B−C64B) may be a result of minor conformational disorder, occupational disorder with the brominated starting material, or handling of the twinning. For **3**, disorder of the butyl chains was modeled as two orientations each with occupancy of 0.5 as determined by refinement before fixing in each case. The butyl chains numbered C51−C54′ were modeled isotropically after anisotropic refinement became unstable. Appropriate restraints were applied to the geometry and displacement parameters of the butyl chains. For **4** atom S44 was found to be disordered over two positions, occupancy summed to unity using a free variable, with appropriate similarity restraints applied to the bond lengths between S44 or S44′ and the adjacent carbon atom. Also for **4**, a C_6H_5Me solvent molecule was found to be disordered over a crystallographic inversion center with further positional disorder, indicated by the Fourier map, which could not be modeled. Appropriate restraints were applied to the geometry and displacement parameters of this C_6H_5Me molecule.

Crystal data for **2**: $C_{52}H_{42}Fe_2N_2O_4$. Monoclinic, space group $C2$, a = 30.9591(9), b = 15.4042(3), c = 21.1507(6) Å, β = 117.241(2)°, V = 8968.0(4) Å^3, Z = 8, D_{calc} = 1.290 g cm^{-3}, μ = 0.693 mm^{-1}, F(000) = 3616. A total of 50313 reflections were collected, of which 19403 were unique, with R_{int} = 0.046. Final R_1 (wR_2) = 0.0966 (0.269) with GOF = 1.03. Flack parameter = 0.16(2).

Crystal data for **3**: $C_{52}H_{42}Fe_2N_2O_4$. Triclinic, space group $P\bar{1}$, a = 12.614(3), b = 12.629(3), c = 13.098(3) Å, α = 83.014(3)°, β = 73.770(3)°, γ = 81.552(3)°, V = 1974.5(9) Å^3, Z = 2, D_{calc} = 1.464 g cm^{-3}, μ = 0.787 mm^{-1}, F(000) = 904. A total of 12789 reflections were collected, of which 5588 were unique, with R_{int} = 0.065. Final R_1 (wR_2) = 0.0693 (0.195) with GOF = 1.00.

Crystal data for **4**: $C_{46}H_{36}Co_2N_2O_4S_4 \cdot 1.5(C_7H_8)$. Triclinic, space group $P\bar{1}$, a = 13.2568(6), b = 13.7187(6), c = 14.9131(7) Å, α = 95.129(1)°, β = 108.214(1)°, γ = 108.376(1)°, V = 2391.2(2) Å^3, Z = 2, D_{calc} = 1.479 g cm^{-3}, μ = 0.920 mm^{-1}, F(000) = 1102. A total of 27294 reflections were collected, of which 14145 were unique, with R_{int} = 0.048. Final R_1 (wR_2) = 0.0538 (0.161) with GOF = 1.04.

Crystallographic data have been deposited with the Cambridge Crystallographic Data Centre as supplementary publications CCDC 731962−731964 for complexes **2**−**4**, respectively.

Electrochemical and Spectroelectrochemical Measurements. CH_2Cl_2 (Fisher) was freshly distilled from calcium hydride under an atmosphere of dinitrogen. Ferrocene (Aldrich) was used as received. Cyclic voltammetric and coulometric studies were carried out using an Autolab PGSTAT20 potentiostat. Standard cyclic voltammetry was carried out under an atmosphere of argon using a three-electrode arrangement in a single compartment cell. A glassy carbon working electrode, a Pt wire secondary electrode, and a saturated calomel reference electrode, chemically isolated from the test solution via a bridge tube containing electrolyte solution and fitted with a porous Vycor frit, were used in the cell. The solutions were 10^{-3} M in test compound and 0.4 M in $[NBu_4][BF_4]$ as supporting electrolyte. Redox potentials are quoted versus the ferrocenium-ferrocene couple used as an internal reference.[19] Compensation for internal resistance was not applied.

Bulk electrolysis experiments, at a controlled potential, were carried out using a two-compartment cell. The Pt/Rh gauze basket working electrode was separated from the wound Pt/Rh gauze secondary electrode by a glass frit. A saturated calomel reference electrode was bridged to the test solution through a Vycor frit orientated at the center of the working electrode. The working electrode compartment was fitted with a magnetic stirrer bar, and the test solution was stirred rapidly during electrolysis.

Solutions were 0.4 M in $[NBu_4][BF_4]$ as supporting electrolyte and 10^{-3} M in test compound and were prepared using Schlenk line techniques. Electrolyzed solutions were transferred to quartz tubes, via steel canula, for analysis by EPR spectroscopy. EPR spectra were recorded on a Bruker EMX spectrometry and simulated using WINEPR SimFonia (Shareware version 1.25, Brüker Analytische Messtechnik GmbH).

The UV/vis spectroelectrochemical experiments were carried out in an optically transparent electrochemical (OTE) cell (modified quartz cuvette, optical path length 0.5 mm).[20] A three-electrode configuration, consisting of a Pt/Rh gauze working electrode, a Pt wire secondary electrode (in a fritted PTFE sleeve) and a saturated calomel electrode, chemically isolated from the test solution via a bridge tube containing electrolyte solution and terminated in a porous frit, was used in

(16) Cernik, R. J.; Clegg, W.; Catlow, C. R. A.; Bushnell-Wye, G.; Flaherty, J. V.; Greaves, N.; Burrows, I.; Taylor, D. J.; Hamichi, M. *J. Synchrotron Radiat*. **1997**, *4*, 279–286.
(17) Cosier, J.; Glazer, A. M. *J. Appl. Crystallogr*. **1986**, *19*, 105.
(18) Sheldrick, G. M. *Acta Crystallogr*. **2008**, *A64*, 112–122.
(19) Gagné, R. R.; Koval, C. A.; Lisensky, G. C. *Inorg. Chem*. **1980**, *19*, 2854.
(20) Macgregor, S. A.; McInnes, E.; Sorbie, R. J.; Yellowlees, L. J. *Molecular Electrochemistry of Inorganic, Bioinorganic and Organometallic Compounds*; Pombeiro A. J. L., McCleverty, J. A., Eds.; Kluwer Academic Publishers: Norwell, MA, 1993; p 503.

Scheme 2. Synthetic Procedures for **2** and **3**[a]

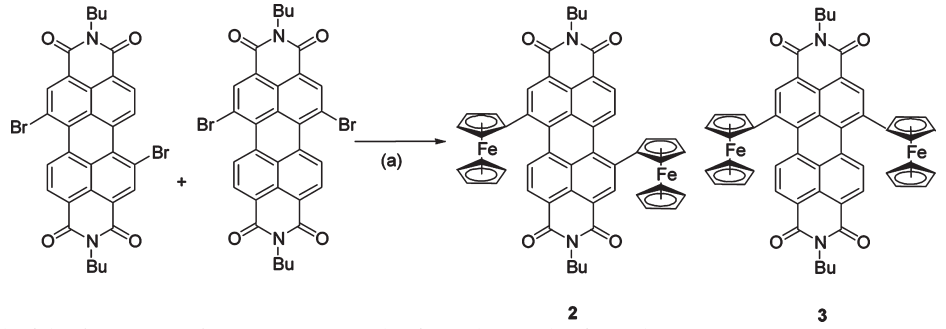

[a] (a) $FcB(OH)_2$, $Pd(PPh_3)_4$, AgO, CsF, toluene, 110 °C, 65% (1,7 isomer), 12% (1,6 isomer).

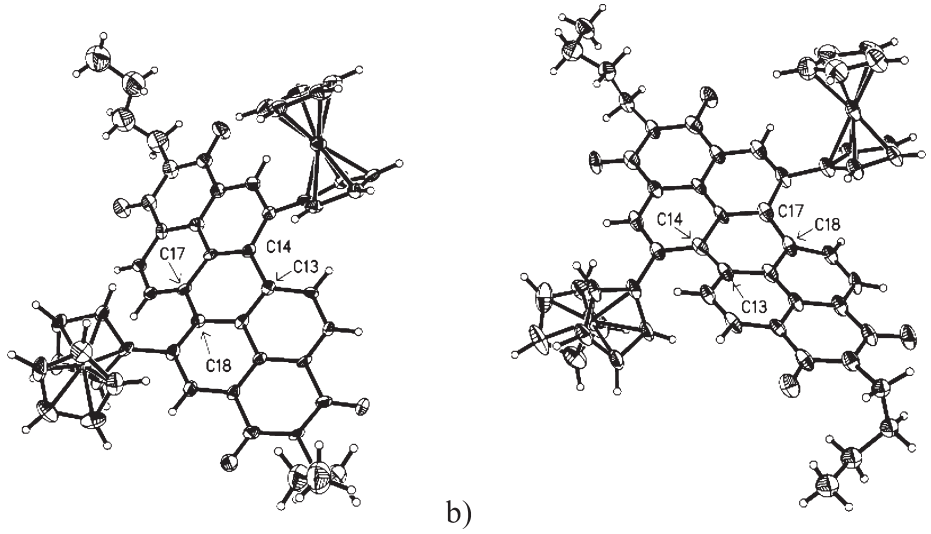

Figure 1. Views of the single crystal structures of compounds **2** (a) and **3** (b) illustrating the twisted arrangement of the perylene core in both the 1,7- and 1,6-isomers of this compound. Displacement ellipsoids are drawn at the 50% probability level. In the case of (a) only one of a pair of independent molecules is shown.

the cell. The potential at the working electrode was controlled by a Sycopel Scientific Ltd. DD10 M potentiostat. The UV/vis spectra were recorded on a Perkin-Elmer Lambda 16 spectrophotometer. The cavity was purged with dinitrogen, and temperature control at the sample was achieved by flowing cooled dinitrogen across the surface of the cell.

Results and Discussion

Synthesis. Compounds **1**−**5** were prepared as outlined in Scheme 1 (**1**, **4**, **5**) and Scheme 2 (**2**, **3**), exploiting Sonagashira coupling in the case of **1**, **4**, and **5** to introduce acetylenyl functionality to the perylene, replacing bromo substituents. For the synthesis of **4**, following the initial introduction of acetylenyl substituents to the perylene core, reaction with S_8 and cyclopentadienylcobalt(I) dicarbonyl affords compound **4** in good yield. Compounds **2** and **3** (Scheme 2) were prepared by the direct Suzuki coupling of $Fc[B(OH)_2]$ in the presence of $Pd(PPh_3)_4$, AgO, and CsF in C_6H_5Me.[21]

In the case of compounds **2** and **3** the 1,7 (**2**) and less commonly studied 1,6 (**3**) isomers were successfully isolated by column chromatography. Preparation of the dibromo-substituted PBI, *N,N*′-bis-(*n*-alkyl)-dibromo-3,4:9,10-perylenetetracarboxylic bisimide, yields a mixture of both 1,7- and 1,6- isomers in an estimated 80:20 ratio which it has not proven possible to separate.[13] The 1,7-isomer is always the major product from the bromination of perylene-3,4:9,10-tetracarboxylic acid and as a result the same isomer is also the major product from substitution reactions using the "as synthesised" *N,N*′-bis-(*n*-alkyl)-dibromo-3,4:9,10-perylenetetracarboxylic bisimide. Thus in this study it was found that only in the case of di-Fc substituted compounds (**2** and **3**) did the isolation of the minor 1,6 isomer (**3**) prove possible. For **1** and **4** the 1,7 isomers could be isolated but unfortunately we were unable to separate pure samples of the corresponding 1,6 isomers. Compound **5** was prepared by utilizing a Sonagashira coupling of phenylacetylene with Br_2−PBI and provided a useful comparison to the other compounds in terms of the redox behavior.

Single Crystal X-ray Diffraction Structural Studies. Single crystals of compounds **2**−**4** were grown by vapor diffusion of C_6H_5Me (**2**, **4**) or *n*-hexane (**3**) into $CHCl_3$ solutions of the respective compounds and X-ray diffraction data collected allowing determination of the conformational arrangement of the molecules in the solid-state (see Figure 1 for views of compounds **2** and **3** and Table 1 for selected bond lengths and angles). The single crystal structures of **2** and **3** represent the first examples of a structurally characterized pair of 1,6- and 1,7-isomers of perylene-bisimides. Both **2** and **3** adopt Fe−C bond

(21) Qiu, W.; Chen, S.; Sun, X.; Liu, Y.; Zhu, D. *Org. Lett.* **2006**, *8*, 5.

Table 1. Selected Bond Lengths (Å), Angles, and Torsion Angles (deg) for **2**, **3**, and **4**

		2	
Fe1−C31A	2.045(6)	Fe2−C41A	2.033(5)
Fe1−C32A	2.045(5)	Fe2−C42A	2.047(5)
Fe1−C33A	2.042(6)	Fe2−C43A	2.049(5)
Fe1−C34A	2.039(5)	Fe2−C44A	2.034(6)
Fe1−C35A	2.042(6)	Fe2−C45A	2.024(5)
Fe1−C36A	2.053(6)	Fe2−C46A	2.037(6)
Fe1−C37A	2.056(6)	Fe2−C47A	2.056(7)
Fe1−C38A	2.049(6)	Fe2−C48A	2.058(7)
Fe1−C39A	2.043(5)	Fe2−C49A	2.040(6)
Fe1−C40A	2.044(6)	Fe2−C50A	2.028(5)
Fe−C(31A−35A) *ave.*	2.043	Fe−C(41A−45A) *ave.*	2.037
Fe−C(36A−40A) *ave.*	2.049	Fe−C(46A−50A) *ave.*	2.044
C13A−C14A	1.477(8)	C17A−C18A	1.482(9)
C12A−C13A−C14A−C1A	−15.8(11)	C14A−C1A−C31A−C35A	135.5(7)
C6A−C17A−C18A−C7A	−18.5(10)	C18A−C7A−C41A−C45A	132.8(6)
Fe3−C31B	2.058(6)	Fe4−C41B	2.048(7)
Fe3−C32B	2.071(6)	Fe4−C42B	2.022(5)
Fe3−C33B	2.058(6)	Fe4−C43B	2.010(6)
Fe3−C34B	2.038(6)	Fe4−C44B	2.029(6)
Fe3−C35B	2.039(6)	Fe4−C45B	2.054(6)
Fe3−C36B	2.056(7)	Fe4−C46B	2.037(6)
Fe3−C37B	2.064(8)	Fe4−C47B	2.036(6)
Fe3−C38B	2.076(8)	Fe4−C48B	2.045(7)
Fe3−C39B	2.075(6)	Fe4−C49B	2.050(7)
Fe3−C40B	2.062(8)	Fe4−C50B	2.044(5)
Fe−C(31B−35B) *ave.*	2.053	Fe−C(41B−45B) *ave.*	2.032
Fe−C(36B−40B) *ave.*	2.066	Fe−C(46B−50B) *ave.*	2.042
C13B−C14B	1.501(11)	C17B−C18B	1.512(12)
C12B−C13B−C14B−C1B	−17.9(13)	C14B−C1B−C31B−C35B	143.9(8)
C6B−C17B−C18B−C7B	−17.3(13)	C18B−C7B−C41B−C45B	132.9(8)
		3	
Fe1−C31	2.036(6)	Fe2−C41	2.063(6)
Fe1−C32	2.051(6)	Fe2−C42	2.052(7)
Fe1−C33	2.047(6)	Fe2−C43	2.048(7)
Fe1−C34	2.051(7)	Fe2−C44	2.028(7)
Fe1−C35	2.024(6)	Fe2−C45	2.029(7)
Fe1−C36	2.038(7)	Fe2−C46	2.063(8)
Fe1−C37	2.046(8)	Fe2−C47	2.027(8)
Fe1−C38	2.055(8)	Fe2−C48	2.041(8)
Fe1−C39	2.040(8)	Fe2−C49	2.030(8)
Fe1−C40	2.040(7)	Fe2−C50	2.047(8)
Fe−C(31−35) *ave.*	2.042	Fe−C(41−45) *ave.*	2.044
Fe−C(36−40) *ave.*	2.044	Fe−C(46−50) *ave.*	2.042
C13−C14	1.466(8)	C17−C18	1.461(9)
C12−C13−C14−C1	−19.6(10)	C14−C1−C31−C35	−46.9(9)
C6−C17−C18−C7	−23.4(9)	C17−C6−C41−C45	−42.6(10)
		4	
Co1−S32	2.1167(8)	Co2−S42	2.1096(7)
Co1−S34	2.1132(8)	Co2−S44	2.1116(11)
Co1−C35	2.052(4)	Co2−C45	2.047(3)
Co1−C36	2.046(4)	Co2−C46	2.048(3)
Co1−C37	2.045(3)	Co2−C47	2.047(4)
Co1−C38	2.055(3)	Co2−C48	2.024(4)
Co1−C39	2.049(3)	Co2−C49	2.026(3)
S42−C41	1.722(3)	S32−C31	1.719(2)
S44−C43	1.706(3)	S34−C33	1.706(3)
C41−C43	1.363(4)	C31−C33	1.369(4)
C13−C14	1.466(3)	C17−C18	1.471(3)
Co1−Cp[a]	1.660	Co2−Cp[a]	1.651
S32−Co1−S34	91.67(3)	S42−Co2−S44	91.62(3)
C12−C13−C14−C1	−21.7(4)	C14−C1−C31−C33	−47.9(4)
C6−C17−C18−C7	−15.3(4)	C18−C7−C41−C43	128.7(3)

[a] Distance between the cobalt cation and the centroid of the Cp ring.

lengths anticipated for the ferrocenyl units with staggered cyclopentadienyl rings, as opposed to ferrocenium species, confirming the oxidation state of the ferrocenyl substituents.

As anticipated for disubstituted perylenetetracarboxylic bisimides, in each case the molecule adopts a twisted arrangement of the perylene core (Figure 1) induced by steric interactions between the substituents and the hydrogen atom located on the adjacent bay region position of the perylene ring. Thus, the perylene core can be considered as two naphthyl moieties linked at the 13/14 and 17/18 positions. Interplanar angles of 22.76/23.63° (**2**) or 21.41° (**3**) are observed between these two naphthyl subunits. The twisting of the two naphthyl subunits is accompanied by the internaphthyl C−C bond lengths being relatively long, 1.477(8)−1.512(12) Å (**2**) or 1.466(8)/1.461(9) Å (**3**), in comparison to average C=C double bond lengths (c.f. 1.41 Å for the average bond length within each naphthyl unit). The ferrocene moieties are positioned on opposing sides of the perylene-bisimide plane such that the cyclopentadienyl group adopts a twisted arrangement, with an interplanar angle of 41.4° (or 47.3°), with respect to the naphthyl group to which each is attached.

The discontinuity in aromaticity across the perylene core in these disubstituted species may be anticipated to reduce electronic communication across the central "aromatic" scaffold. However, there are noticeable differences between some of the molecules. In particular, compound **3** represents the first structurally characterized example of a 1,6-disubstituted perylenetetracarboxylic bisimide and has both substituents attached to the same naphthyl moiety, thereby reducing the implications of the perylene twist such that a clear aromatic pathway between the two Fc subunits is maintained in the molecule.

Compound **4** crystallizes as a toluene solvate in the triclinic space group $P\bar{1}$. As with **2** and **3**, the perylene core is twisted with an interplanar angle of 21.23° between these two naphthyl subunits and is accompanied by the observation of relatively long C−C bonds between the two naphthyl groups 1.466(3)/1.471(3) Å (see Figure 2 for a view of compound **4** and Table 1 for selected bond lengths and angles). The (Cp)Co-dithiolene moieties are positioned on adjacent sides of the perylene-bisimide plane such that the dithiolene group (CoS_2C_2) adopts a twisted arrangement with an interplanar angle of 47.8° (or 54.7°) with respect to the naphthyl group to which each unit is attached. Inspection of the bond lengths and angles of the Co-dithiolene moiety (Table 1) indicates that the formal cobalt(II) center and dithiolene ligand adopt a geometry similar to that reported for the analogous phenyl substituted dithiolene, [CpCo(S_2C_2(H)Ph)],[22] indicating an ene-dithiolate arrangement of the dithiolene moiety.

The solid-state structures of perylenetetracarboxylic bisimides have a significant effect on the properties of the compounds, leading to conductivity in particular.[23] Compounds **2**−**4** all adopt restricted stacked arrangements because of the disubstituted nature of each compound, such that the extended stacks observed for unsubstituted perylenetetracarboxylic bisimides[10b] are not observed.

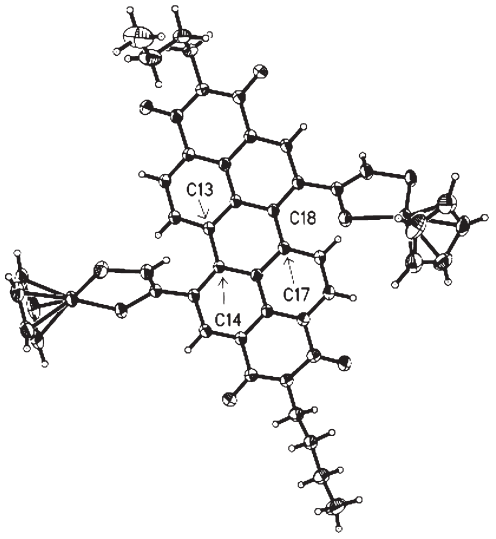

Figure 2. Views of the single crystal structures of compound **4** illustrating the twisted arrangement of the perylene core. The relative orientations of the Co-dithiolene moieties in the solid state are also illustrated. Displacement ellipsoids are drawn at the 50% probability level.

Compound **2** adopts $\pi-\pi$ interactions between adjacent molecules to form pairs of stacked molecules with the Fc groups oriented such that they protrude from the opposing faces of the stacked pairs (Figure 3a) (centroid···centroid separations between nearest-neighbor naphthyl aromatic rings 3.70, 3.64, 3.64, 3.73 Å). In contrast to **2**, compound **3** adopts an extended stack via the formation of $\pi-\pi$ interactions (Figure 3b). Because of the relative arrangement of the Fc groups in **3**, being the disubstituted 1,6-isomer, the molecule is non-centrosymmetric with one-half of the molecule Fc substituted and the other half unsubstituted. The molecules stack such that the unsubstituted ends of the molecule are $\pi-\pi$ stacked with the unsubstituted end of an adjacent molecule interacting via naphthyl moieties forming pairs of molecules (centroid···centroid separations between nearest-neighbor aromatic rings 3.71 Å). These pairs of molecules also interact through the Fc-substituted ends of each molecule such that the imide moieties of each molecule are stacked with the adjacent imide group (centroid···centroid separation 3.55 Å). Thus, through a combination of two different interactions extended stacks are observed in the solid-state structure of **3**.

In a similar manner to **2**, compound **4** also exhibits pairs of stacked molecules but with $\pi-\pi$ interactions between adjacent imide rings (centroid···centroid separation 3.62 Å). Within each molecule one imide ring participates in $\pi-\pi$ interactions with another molecule of **4** while the other imide ring in the molecule forms a $\pi-\pi$ interaction with a guest toluene solvent molecule (centroid···centroid separation 3.57 Å), thereby precluding extension of the $\pi-\pi$ stack beyond a dimeric unit.

Electrochemical Studies. Cyclic voltammetry was used to assess the redox behavior of compounds **1a**−**5** and to establish the influence of the redox active, ferrocenyl or cobalt-dithiolene appendages attached to the perylene-bisimide cores. As a result of enhanced solubility the dioctyl derivatized version of **1**, *N*,*N*′-di-(*n*-octyl)-1,7-diethynylferrocenyl-perylene-3,4:9,10-tetracarboxylic acid bisimide **1a**, was used for electrochemical, spectroelectrochemical

(22) Periyasamy, G.; Burton, N. A.; Hillier, I. H.; Vinccent, M. A.; Disley, H.; McMaster, J.; Garner, C. D. *Faraday Discuss.* **2007**, *135*, 469–488.

(23) Chen, Z.; Stepanenko, V.; Dehm, V.; Prins, P.; Siebbeles, L. D. A.; Seibt, J.; Marquetand, P.; Engel, V.; Würthner, F. *Chem.—Eur. J.* **2007**, *13*, 436.

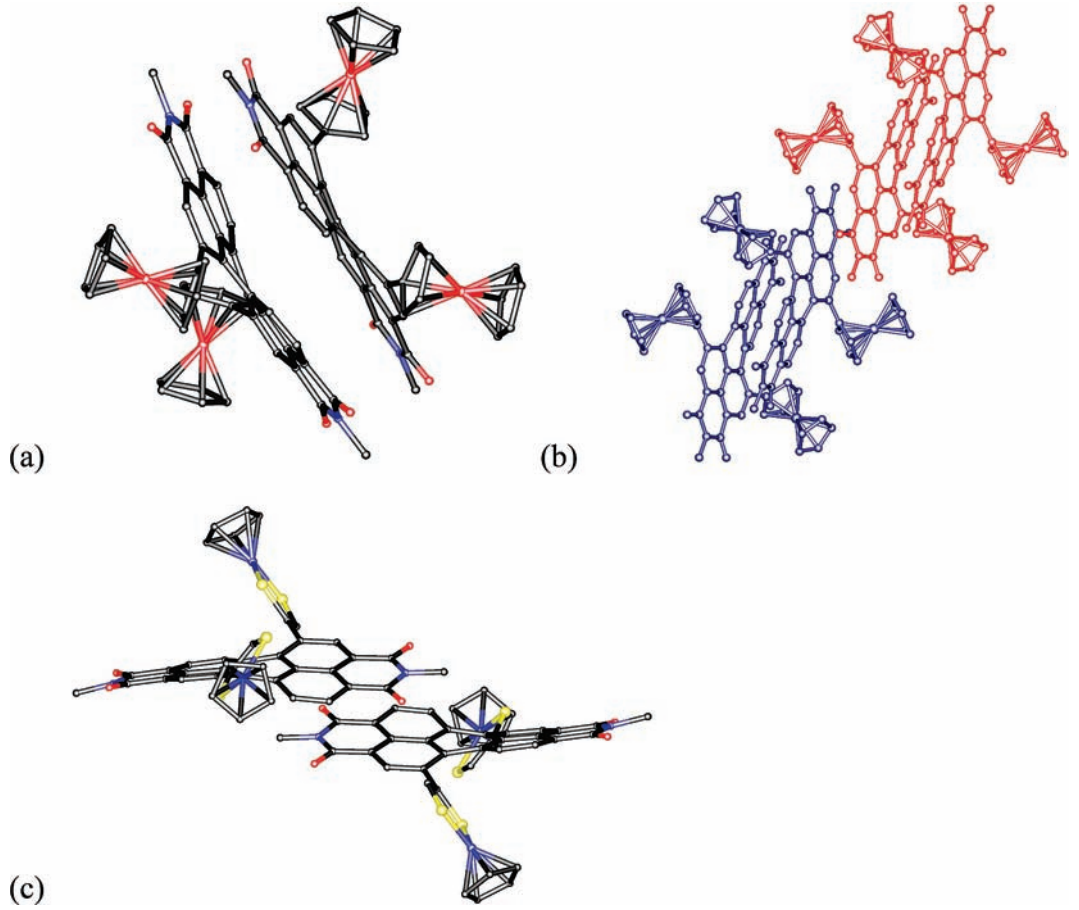

Figure 3. View of the stacking between adjacent molecules observed in the structures of (a) **2**, (b) **3**, and (c) **4**. Note the formation of dimeric pairs in each case but in the case of **3**, 1,6-$(Fc)_2$-PBI, dimeric pairs are in turn stacked to form extended one-dimensional arrays.

and EPR studies. The replacement of *n*-butyl by *n*-octyl at the imide nitrogen is not anticipated to make any difference to the electrochemical properties of the compound because of the node in the HOMO at the nitrogen atoms of the two imide functions.[12]

Cyclic voltammograms recorded for compounds **1a** and **5** (Figure 4), **2**, **3**, and **4** (Figure 5) and Table 2 for pertinent electrochemical data. The reduction processes of all four compounds follow the same trends reported for other perylene-bisimide compounds.[9] Hence, all the compounds undergo two reversible one-electron reduction processes based on the perylene core (Figures 4, 5). Trends in reduction potentials correspond to the electron withdrawing or donating nature of the group attached to the perylene-bis-(dicarboximide) framework and, as demonstrated by **2** and **3**, the position of bay-substitution on the perylene core has only a small effect on these potentials. For **2** and **3**, the ferrocenyl group (σ_p: −0.15)[24] donates electron density relative to the acetylene linker in **1** and 1,7-$(C{\equiv}CPh)_2$-PBI, prepared as a model complex (for CCPh σ_p: +0.14): as a result, reduction processes occur at slightly more negative potentials. Given the similarity between potentials of the first and second reductions of 1,7-$(C{\equiv}CPh)_2$-PBI and compound **4**, it would appear that the CpCo(dithiolene) moiety acts as an electron withdrawing moiety.

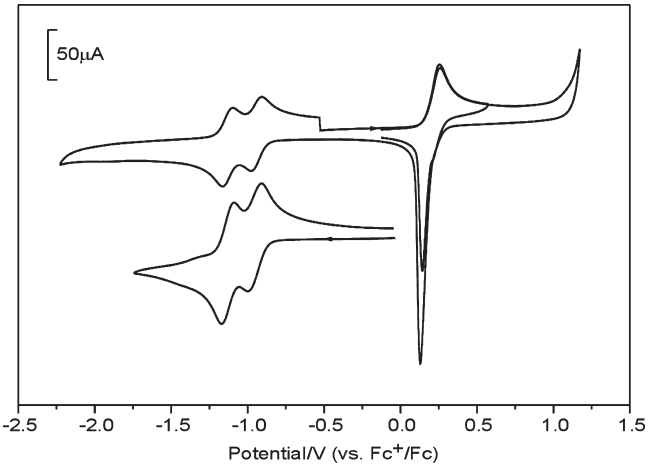

Figure 4. Cyclic voltammograms recorded for **1a** (top) and **5** (bottom) in CH_2Cl_2 containing $[Bu_4N][BF_4]$ (0.4 M) at 0.1 V s^{-1}.

In the case of the ferrocenyl substituted compounds **1a**−**3** the oxidation processes associated with the ferrocenyl groups is of particular interest. The oxidation of **1a** (Figure 4) was determined by coulometry to be a two-electron process, and given the nature of the molecule and potential of oxidation (perylenes usually oxidize at significantly greater potentials,[25] unless substituted by

(24) Hansch, C.; Leo, A.; Taft, R. W. *Chem. Rev.* **1991**, *91*, 165–195.

(25) Lee, S. K.; Zu, Y.; Herrmann, A.; Geerts, Y.; Müllen, K.; Bard, A. J. *J. Am. Chem. Soc.* **1999**, *121*, 3513–3520.

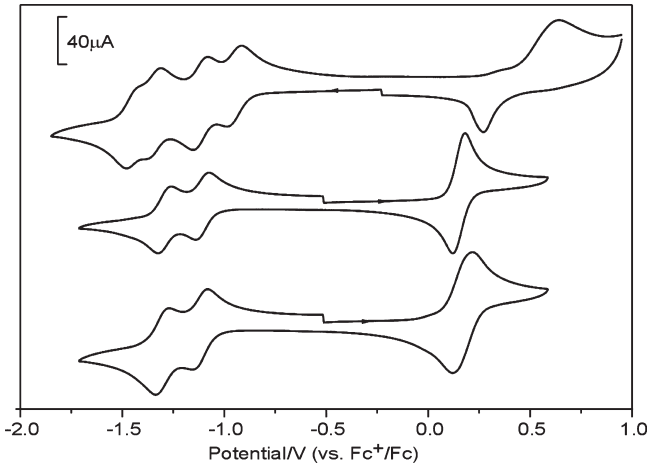

Figure 5. Cyclic voltammograms recorded for **4** (top), **2** (middle), and **3** (bottom) in CH_2Cl_2 containing $[Bu_4N][BF_4]$ (0.4 M) at 0.1 V s^{-1}.

Table 2. Electrochemical Data for Disubstituted PBI Derivatives[a]

compound	1st reduction	2nd reduction	oxidation	$\Delta E(Fc^+/Fc)$
1a	−0.94 (0.07)	−1.13 (0.07)		(0.07)
2	−1.11 (0.07)	−1.29 (0.07)	+0.15 (0.07)	(0.07)[b]
3	−1.12 (0.07)	−1.31 (0.06)	+0.17 (0.09)	(0.08)[b]
4	−0.96 (0.07)	−1.12 (0.08)[c]	d	(0.07)
5	−0.96 (0.10)	−1.13 (0.09)		(0.09)

[a] All potentials reported as $E_{1/2}$ (= $(E_p^a + E_p^c)/2$) in V vs Fc^+/Fc at 0.1 Vs^{-1} scan rate and quoted to the nearest 0.01 V. Values in parentheses are ΔE (= $E_p^a - E_p^c$) for the couple at 0.01 Vs^{-1}. [b] [Fe$(C_5Me_5)_2$] (Fc*) used as internal standard: $E_{1/2}$ Fc^{*+}/Fc^* vs $E_{1/2}$ Fc^+/Fc was −0.52 V by independent calibration under identical conditions. [c] In addition two further reduction couples were observed but were too closely overlapped to be resolved by cyclic voltammetry; however, these were resolved by square wave voltammetry as peaks at −1.34 and −1.44 V (the 1st and 2nd reductions were −0.94 and −1.10 V, respectively by square wave voltammetry). [d] Oxidation process at E_p^a 0.65 V with corresponding reduction at 0.27 V.

N-donor groups),[26,10b] this was assigned to the simultaneous oxidation of the two ferrocene groups.[10a,11] Additionally, under the conditions of study 1,7-(C≡CPh)$_2$-PBI **5** (Figure 4) does not exhibit an oxidation process. The unusual form of the cyclic voltammogram was ascribed to oxidation followed by deposition of the generated ferrocenium salt on the surface of the working electrode. In the first half-cycle, a single anodic waveform was observed for which I_p^a was proportional to (scan rate)$^{1/2}$ (R^2 = 0.987). In the second half-cycle, corresponding to the reduction of the electro-generated salt, two waves are observed, the intensities of which are scan rate, and hence time scale, dependent. At faster scan rates, corresponding to shorter time scales, a process at more positive potential dominated; this was assigned to the reduction of the ferrocenium salt in solution.

At slower scan rates, a reduction at slightly lower potential was more intense and showed significant current variation with scan rate. This was attributed to the precipitated salt being stripped off the electrode surface. Evidence for this came from coulometry, where it was observed that as the oxidation progressed, a dark solid coated the electrode. Spectroelectrochemistry showed this process to be chemically reversible; oxidation resulted in a significant drop in intensity across the spectral range, corresponding to the oxidation and subsequent loss of chromophore from solution, while reduction regenerated the original spectral profile of $[\mathbf{1a}]^0$ almost exactly.

Of interest was the difference between the physical properties, upon oxidation, of **1a** (Figure 4) and the compounds **2** and **3** (Figure 5). While oxidation of **1a** yielded an insoluble product, which reflected in the waveform obtained for the cyclic voltammogram (Figure 4 and Supporting Information), both **2** and **3** appeared to give soluble products upon oxidation; hence the cyclic voltammogram comprised a single wave both in the forward and reverse cycle of the ferrocenylium/ferrocenyl couple.

The oxidation of both **2** and **3** was determined, by coulometry and UV/vis spectroelectrochemistry at 243 K, to be a two-electron, chemically reversible process assigned as the oxidation of the ferrocenyl groups. The small positive shift in oxidation potential for both **2** and **3** with respect to unsubstituted ferrocene is consistent with substitution of one ferrocenyl cyclopentadienyl ring by an electron withdrawing moiety. Only a small variation between the potential of oxidation for **2** and **3** was observed, with **2** slightly easier to oxidize.

More interestingly the behavior of the oxidation couple for **2** and **3** with variation in scan rate revealed a small degree of communication between the two ferrocenyl substituents (Figure 5). For **3**, the waveshape appeared broad with ΔE (= $E_p^a - E_p^c$) values considerably higher than those of Fc*, bis-(pentamethylcyclopentadienyl)iron(II), used as the internal standard. We interpret this broad shape as resulting from the close overlap of two oxidation processes, one on each ferrocenyl, occurring at slightly different potentials: this is a consequence of communication through the naphthalene linker between the ferrocene centers, although the absence of two resolved waves would suggest the extent of this communication to be small. This contrasts with the oxidation behavior of **2** which, at a scan rate of 0.1 V s^{-1}, gave separation between the forward and reverse waves of the oxidation cycle consistent with that of the internal standard. However, as the scan rate was lowered, ΔE dropped below that of Fc* under identical conditions, such that, at 0.01 V s^{-1}, the separation was 55 mV, below the value expected for a one-electron reversible couple (ca. 70−80 mV as observed for the internal standard) and less than that expected for two one-electron reversible couples that show no communication. This small value of ΔE may result from a genuine two-electron reversible process, with ΔE larger than the theoretical value of 30 mV. The tentative assignment of this process as two sequential one-electron oxidation processes, that is, an EE process, with these characteristics would mean that the oxidation, which occurs on two different groups (but with equivalent orbitals) in the molecule results in these groups interacting attractively (i.e., ΔE^o (= $E_{ox1} - E_{ox2}$) > 35.6 mV) which would require a large structural rearrangement, or a large solvation effect or ion pairing as a result of the first

(26) (a) Lukas, A. S.; Zhao, Y.; Miller, S. E.; Wasielewski, M. R. *J. Phys. Chem. B* **2002**, *106*, 1299–1306. (b) Zhao, Y.; Wasielewski, M. R. *Tetrahedron Lett.* **1999**, *40*, 7047–7050. (c) Ahrens, M. J.; Tauber, M. J.; Wasielewski, M. R. *J. Org. Chem.* **2006**, *71*, 2107–2114. (d) Tauber, M. J.; Kelley, R. F.; Giaimo, J. M.; Rybtchinski, B.; Wasielewski, M. R. *J. Am. Chem. Soc.* **2006**, *128*, 1782–1783.

Table 3. EPR Data for Disubstituted PBI Derivatives **1**−**5** in Reduced States[a]

compound	g_{iso}	$a_{iso}/\times10^{-4}$ cm^{-1} [b]
$[\mathbf{1a}]^-$	2.004	1.51 (a_{2H}), 0.59 (a_{2H}), 0.55 (a_{2H}), 0.52 (a_{2N})[c]
$[\mathbf{2}]^-$	2.005	1.23 (a_{2H}), 0.63 (a_{4H}), 0.63 (a_{2N})[d]
$[\mathbf{3}]^-$	2.005	1.22 (a_{2H}), 0.62 (a_{4H}), 0.58 (a_{2N})[e]
$[\mathbf{4}]^-$	2.010	f
$[\mathbf{4}]^{4-}$	2.004	f
$[\mathbf{5}]^-$	2.003	f

[a] In CH_2Cl_2 containing $[^nBu_4N][BF_4]$ (0.4 M) at 298 K unless stated otherwise. [b] Simulation of experimental parameters. [c] Lorentzian line shape and 0.35 G line width. [d] Gaussian line shape and 0.7 G line width. [e] Gaussian line shape and 0.57 G line width. [f] Unresolved.

electron transfer step.[27] However, we do not discount the existence of other mechanisms to explain the observed behavior.

Compound **4** gave a redox process consistent in behavior with the presence of a CpCo(dithiolene) manifold (oxidation at E_p^a 0.65 V and an associated reduction at E_p^c 0.27 V, vs Fc^+/Fc at 0.1 V s^{-1});[28] this was not further studied. However, reduction processes observed for **4** are of considerable interest with a total of four reduction processes observed (Figure 5). The third and fourth reductions are unique to **4** and are assigned as two one-electron reductions on the CpCo(dithiolene) units, the potentials of which are consistent with literature values.[28] Potentials of the third and fourth reductions were resolved by square wave voltammetry and show a difference of about 0.1 V, indicating communication between the two redox centers. Significant communication between these centers contrasts with the behavior of **2** and **3** upon oxidation; hence, communication between the two Co centers would appear to be facilitated by changes occurring in the perylene framework upon double reduction.

EPR Studies. The electrochemical one-electron reduction of each compound produced paramagnetic species. As fluid solutions at ambient temperature, EPR spectroscopy gave signals consistent with the generation of the radical anions, see Table 3. Hyperfine splittings were observed for **1a**, **2**, and **3** (see Figure 6 and Supporting Information); each of which was simulated by the coupling of the unpaired electron to the nucleus of six hydrogen atoms, presumably those of the perylene core, and two nitrogen atoms.[20] For both **4** and **5**, one electron reduction yielded spectra with no or only poorly defined hyperfine splitting.

Two electron reductions of **1a**−**4** yield the corresponding dianionic species, all of which are dark blue. These solutions were essentially EPR silent, with only residual signals present relative to their monoanion analogues (3−18%). For **4**, further reduction at potentials beyond the fourth process regenerated an EPR active species: upon cooling to 77 K, this species gave a spectrum consistent with an unpaired electron coupled to a Co

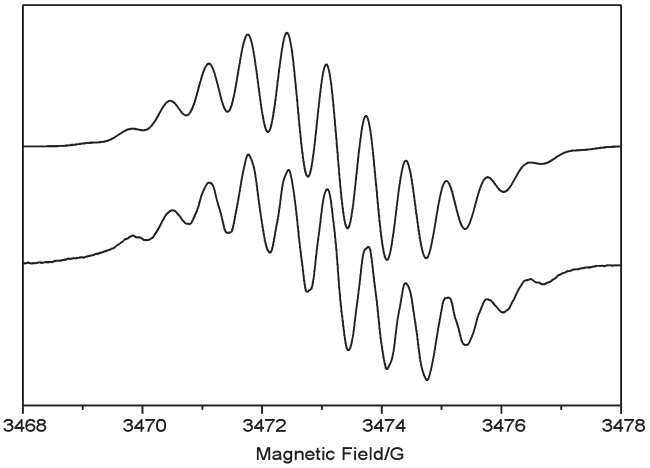

Figure 6. Experimental (bottom) and simulated (top) EPR spectra for electrochemically generated $\mathbf{3}^-$ in CH_2Cl_2 containing $[Bu_4N][BF_4]$ (0.4 M) at 291 K.

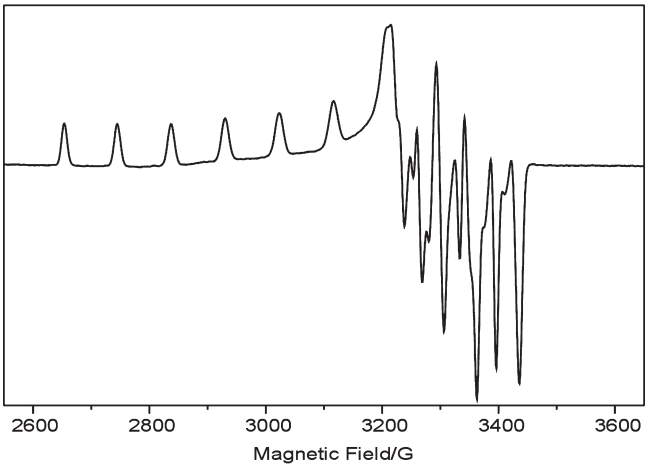

Figure 7. Experimental EPR spectra for electrochemically generated $\mathbf{4}^{4-}$ in CH_2Cl_2 containing $[Bu_4N][BF_4]$ (0.4 M) at 77 K.

nucleus (I = 7/2; see Figure 7), the spectral profile of which was very similar to literature reports of other [CpCo(dithiolene)] moieties.[29] However, reproduction of all the features in the experimental spectrum was not achieved by simulation using rhombic parameters, a point noted previously for the EPR spectrum of [CpCo(pyridine-4-yl-ene-1,2-dithiolate)]$^-$ recorded at X- and Q-band frequencies as a frozen glass in tetraethylene glycol at 77 K, and a consequence of the non-coincidence of A and g tensors giving a monoclinic EPR symmetry.[30]

Spectroelectrochemistry. In situ one- and two-electron reductions of **1a**−**5** were followed by UV/vis/nIR spectroelectrochemistry at an optically transparent electrode. The one-electron reduced radical anions show major bands which are red-shifted relative to their parent molecules, with series of transitions extending into the nIR region. The second reduction blue-shifts the spectra with respect to those of the radical anion, with the most intense transitions for **1a** (634 nm), **2** (630 nm), **3** (628 nm), and **5** (639 nm) all occurring at similar wavelengths, a result

(27) Bard, A. J.; Faulkner, L. R. *Electrochemical Methods, Fundamentals and Applications*, 2nd ed.; Wiley: New York; pp 505−507.

(28) (a) Ushijima, H.; Kajitani, M.; Smimizu, K.; Satô, G. P.; Akiyama, T.; Sugimori, A. *J. Electroanal. Chem.* **1991**, *303*, 199–209. (b) Kajitani, M.; Akiyama, T.; Sugimori, A.; Hirakata, K.; Hoshina, Y.; Satsu, Y.; Sato, G. P.; Shimizu, K. *J. Electroanal. Chem.* **1988**, *251*, 421–428.

(29) (a) Takayama, C.; Kijitani, M.; Sugiyama, T.; Akiyama, T.; Shimizu, K.; Sugimori, A. *Organometallics* **1997**, *16*, 3498–3503. (b) Hartigan, H. J.; Seeber, G.; Mount, A. R.; Yellowlees, L. J.; Robertson, N. *New J. Chem.* **2004**, *28*, 98–103.

(30) Mabbs, F. E.; Collison, D. *Electron Paramagnetic Resonance of d Transition Metal Compounds*; Elsevier: Amsterdam, 1992; Chapter 7.

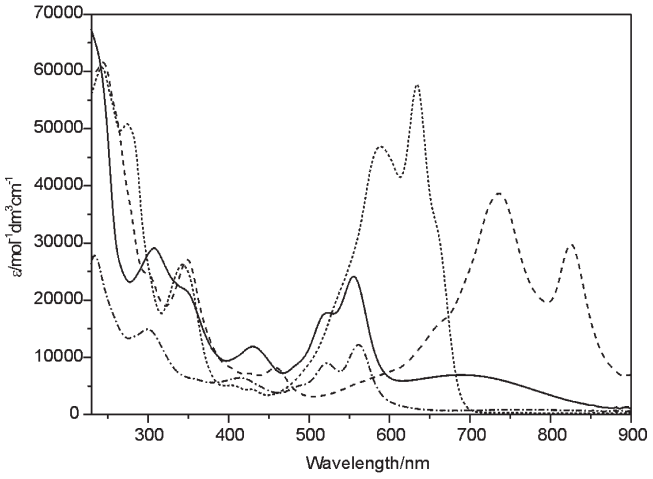

Figure 8. UV−visible spectra recorded in CH_2Cl_2 containing $[Bu_4N][BF_4]$ (0.4 M) using spectroelectrochemical methods for **1a** at 273 K. The spectrum of **1a** is represented by the solid line, $\mathbf{1a}^-$ (dashed line), $\mathbf{1a}^{2-}$ (short dashed line), and the oxidized species $\mathbf{1a}^{2+}$ (dashed-dotted line).

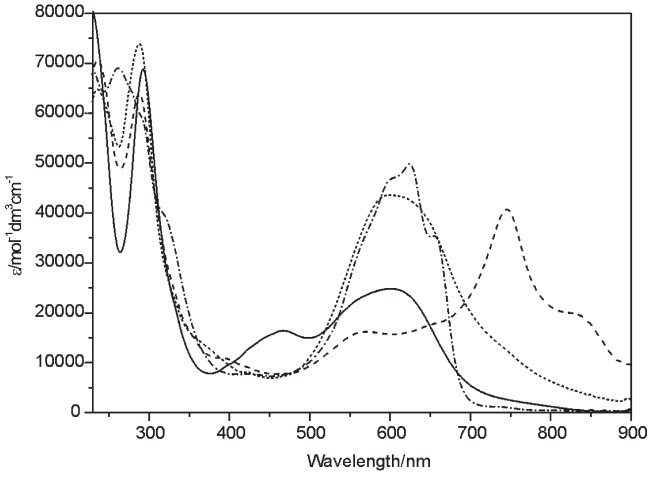

Figure 9. UV−visible spectra recorded in CH_2Cl_2 containing $[Bu_4N][BF_4]$ (0.4 M) using spectroelectrochemical methods for **4** at 273 K. The spectrum of **4** is represented by the solid line, $\mathbf{4}^-$ (dashed line), $\mathbf{4}^{2-}$ (short dashed line), and $\mathbf{4}^{4-}$ (dashed-dotted line).

consistent with other bisimide perylene compounds. Representative UV spectra for the reduced and oxidized states for compound **1a** are shown in Figure 8, while spectra for **2**, **3**, and **5** and representative spectra revealing sharp isosbestic points for the oxidative and reductive transitions of compound **3** are given in the Supporting Information, as is a full tabulated list of adsorption maxima for all oxidation states of **1a**−**5**.

For **4**, the transitions in the visible region appear broad, at least for the dianionic redox state (Figure 9). This may result from the overlap of two strongly absorbing chromophores; those transitions associated with the neutral, anionic and dianionic bisimide perylene core combined with transitions of the [CpCo(dithiolene)] moiety, usually found at about 580 nm. Reduction of the [CpCo(dithiolene)] unit depletes this transition; hence, fully reduced **4** has a less broad appearance to the visible spectral profile and as such is more similar to those of the dianionic species of **1a**, **2**, and **3**.

Conclusions

A series of difunctionalized perylene-bisimides has been synthesized, structurally characterized by single crystal X-ray diffraction methods, and their optical and redox properties investigated. Compounds **1**−**4** represent multistate redox-active architectures with two redox-active ferrocene or cobalt-dithiolene moieties introduced into the "bay" region of the perylene-bisimide core. Structural characterization of **2**−**4** confirms the anticipated twisted nature of the central perylene core. Compounds **2** and **3** represent the first pair of disubstituted perylene-bisimide 1,7- and 1,6-isomers with similar degrees of twisting of the perylene core in both cases, 23.2° (ave. for **2**) vs 21.41° (**3**). Structural characterization of **4** also reveals the expected twisting of the perylene core and confirms the ene-dithiolate geometry of the cobalt dithiolene moiety.

Cyclic voltammetry measurements, coupled with spectroelectrochemical and EPR studies, of **1a**−**4**, where **1a** is *N*,*N*′-di-(*n*-octyl)-1,7-diethynylferrocenyl-perylene-3,4:9,10-tetracarboxylic acid bisimide, reveal the two anticipated perylene-bisimide based reductions. The ferrocene substituted compounds **1a**−**3** also display a single reversible two-electron oxidation, with only a small degree of communication between the ferrocene groups observed in the 1,6-isomer where the two ferrocene groups are attached to the same naphthyl moiety. In the case of **4** two reversible reductions associated with the cobalt-dithiolene moieties are observed, confirming communication across the reduced perylene core.

These studies reveal that in designing multistate redox-active architectures using perylene-bisimides the isomeric arrangement of the redox-active appendages has to be considered with 1,6-isomers exhibiting a greater tendency toward communication across the perylene core, facilitated by a single naphthyl group. However, the introduction of groups capable of further reductive processes, such as the cobalt-dithiolene moieties, also facilitates communication across the perylene subunit, presumably as a result of the reduced nature of the perylene core at the potentials required for cobalt-dithiolene reduction. In summary, we have successfully prepared multistate redox-active architectures based upon "bay"-functionalized perylene-bisimides.

Acknowledgment. We would like to gratefully acknowledge the support of the Engineering and Physical Sciences Research Council (EP/D048761/1) and the EU through the NANOMESH STRP NMP4-CT-2004-013817 for funding. We thank the National Crystallography Service at the University of Southampton, U.K., for data collection and STFC for access to SRS Station 9.8.

Supporting Information Available: Supporting Information includes additional figures and data for cyclic voltammograms, EPR spectra, spectroelectrochemistry and X-ray crystallographic files (CIF) are available. This material is available free of charge via the Internet at http://pubs.acs.org.